A Quantitative Treatment of Particle Size Distributions in Emulsion Polymerization

DONALD C. SUNDBERG,* *Department of Chemical Engineering, University of Idaho, Moscow, Idaho 83843*

Synopsis

A quantitative analysis is presented for predicting the particle size distributions obtained in emulsion polymerization. The results obtained are compared with experimental data in terms of the particle-size-distribution curves as well as the statistical parameters of the distributions. Comparisons are made for changes in initiator level, surfactant level, water:monomer ratio, and temperature. The manner in which these variables change the distributions and the reasons for these changes are identified. The distribution of radicals among particles of different sizes is seen to be significant. Large particles are expected to contain a greater number of radicals per particle than the smaller ones in the same latex. The effects of such a radical distribution upon the properties of the latex are discussed.

INTRODUCTION

Particle size and molecular weight distributions of synthetic latices are detailed blueprints of the series of events which embody the process of emulsion polymerization. These distributions are direct results of the controlling parameters of the reaction, and their investigation provides a means of critically evaluating one's understanding of the process. It stands to reason then that the ability of forecasting these distributions, in a fashion which is free from prior assumptions of the form of the distributions themselves, would be a useful tool to both the practitioner and the researcher. The intent of this paper is to present such an approach for the quantitative prediction of particle size distributions in emulsion polymerization. A further publication will present the sequel for the molecular weight distribution.

Only a small portion of the emulsion polymerization literature has been devoted to the subject of particle size distributions. This is undoubtedly due to the difficulties involved in either experimental or theoretical investigations of this parameter. Even for the well-studied polystyrene system, Gerrens's[1] work provides one of the few extensive sets of experimental results showing the influence of recipe and temperature changes upon the resultant particle size distributions. On the theoretical side, contributions have been made by Gardon,[2] O'Toole,[3] Watterson and Parts,[4] Sundberg,[5] and most recently by Min and Ray.[6]

The discussion which follows is largely based on the work accomplished in Ref. 5 and is meant to offer some rather interesting implications of Harkins' mechanistic concepts[7] of the emulsion polymerization process.

* Present address: Department of Chemical Engineering, University of New Hampshire, Durham, N.H. 03824.

Journal of Applied Polymer Science, Vol. 23, 2197–2214 (1979)

0021-8995/79/0023-2197$01.00

QUANTITATIVE DESCRIPTION

The development which follows will make use of the standard reaction mechanisms of free radical polymerization:

$$I \xrightarrow{k_d} 2R\cdot \qquad \text{Initiation}$$

$$R\cdot + M \xrightarrow{k_i} M_1\cdot$$

$$M_n\cdot + M \xrightarrow{k_p} M_{n+1}\cdot \qquad \text{Propagation}$$

$$M_n\cdot + \text{CTA} \xrightarrow{k_{tr,\ \text{CTA}}} P_n + M_1\cdot \qquad \text{Chain transfer}$$

$$M_n\cdot + M_m\cdot \xrightarrow{k_t} P_{n+M} \qquad \text{Termination}$$

where I represents the initiator, $R\cdot$ are the primary radicals, M is the monomer, $M_n\cdot$ are the polymer radicals of length n, CTA is the chain transfer agent (may be monomer, polymer, regulating agent), and P_n represents the dead polymer chains. Since the latex system is heterogeneous, the concentrations of the above species must be defined relative to the appropriate phase volume (i.e., I and $R\cdot$ to the water phase, and the remainder to the oil phase). The rate constants are those for decomposition, initiation, propagation, chain transfer, and chain termination by combination, respectively.

The heterogenous nature of the latex system makes it necessary to consider a fairly large number of assumptions even for the simplest model. Most of these result from the utilization of Harkins's mechanism and the Smith-Ewart case II to describe the process. The present discussion is limited as follows:

isothermal, batch reactor operation
particles absorb radicals from the aqueous phase at a rate proportional to their *surface area*
no radical desorption from the particles
no particle coalescence
monomer and polymer are mutually soluble

Model Development

Although size differences between particles are considered, it is assumed that no particle will contain more than a single free radical.* With this in mind, it is possible to describe the particle-size-distribution frequency function, $N_i(r^3,t)$, by

$$\int_x^y N_i'(r^3,t)\, \mathrm{d}(r^3) \equiv \text{Total number of particles between sizes } x \text{ and } y \text{ which contain } i \text{ radicals}$$

$$\int_x^y N_T'(r^3,t)\, d(r^3) \equiv \text{Total number of particles in system between sizes } x \text{ and } y$$

where $N_T'(r^3,t) = N_1'(r^3,t) + N_0'(r^3,t)$ and $N_i'(r^3,t)$ has the dimensions of moles (of particles†) $(\text{liter}_{H_2O})^{-1}\ (r^3)^{-1}$. The reason that the particle number is written as a function of the particle radius cubed $(r^3)^{-1}$ and time (t) is that the resulting equations are more easily solved using r^3 rather than r. This is discussed more fully in the Appendix.

* Models without this restriction have been developed in Ref. 5.

† A "mole of particles" is taken to be 6.023×10^{23} (or Avagadros number) particles and is used merely for convenience.

The consideration of the size distribution allows one to write the combined surface area of the polymer particles (per liter of water) as

$$A_p = 4\pi N_{Av} \int_{r_m^3}^{\infty} r^2 N'(r^3,t)\, d(r^3) \tag{1}$$

and the total surface area per liter of water S' as that of the micelles plus the polymer particles,

$$S' = 4\pi r_m^2 N_{Av} m + A_p \tag{2}$$

where N_{Av} is Avogadros' Number, r_m is the radius of the micelles, and m is the number of micelles (moles/liter of water).*

At this point, population balances must be written for the active and inactive polymer particles. Following Behnken et al.,[8]

Rate of change in the number of active particles in size range x to y	= Rate at which particles grow into size range at x	−	Rate at which particles grow out of size range at y
	+ Rate at which particles shift populations due to absorbance of a free radical from the aqueous phase		

In the nomenclature set forth here, for particles containing one growing radical, this balance becomes

$$\frac{\partial}{\partial t} \int_x^y N_1'(r^3,t)\, d(r^3) = H(x,t) - H(y,t) + R \frac{4\pi N_{Av}}{S'} \int_x^y r^2 [N_0'(r^3,t) - N_1'(r^3,t)]\, d(r^3)$$

Here R is taken to be the total rate of free radical generation in the aqueous phase.

The rate at which particles grow past size r^3 may be written as

$$H(r^3,t) = N_1'(r^3,t) \frac{d(r^3)}{dt}$$

$N_1'(r^3)$ is used here because only the active particles grow. The rate of volumetric growth of a polymer particle, $d(r^3)/dt$, has been developed by Gardon[9] as

$$\frac{d(r^3)}{dt} = Ki$$

where

$$K = (3/4\pi)(k_p/N_{Av})(d_m/d_p)[\theta/(1-\theta)] \times 10^3$$

and i = number of radicals in a growing particle. Here k_p is propagation rate constant, d_m and d_p are the densities of monomer and polymer, θ is the volume fraction monomer in the particle, and 10^3 is simply the conversion factor between cm^3 and liters (required when k_p is expressed in liters and r in cm). For this model, $i = 1$ and

$$H(r^3) = KN_1(r^3,t)$$

* Computations for m and r_m are shown in the Appendix.

But

$$H(x,t) - H(y,t) = -\int_x^y \frac{\partial(KN_1'(r^3,t))}{\partial(r^3)}\, d(r^3)$$

by definition, and the population balance can be written as

$$\int_x^y \left\{ \frac{\partial N_1'(r^3,t)}{\partial t} + K\frac{\partial N_1'(r^3,t)}{\partial(r^3)} - R\frac{4\pi N_{Av}}{S'} r^2[N_0'(r^3,t) - N_1'(r^3,t)] \right\} d(r^3) = 0$$

Since the integrand vanishes for an arbitrary size interval (x,y), it must be identically zero, leading to

$$\frac{\partial N_1'(r^3,t)}{\partial t} = -K\frac{\partial N_1'(r^3,t)}{\partial(r^3)} + R\frac{4\pi N_{Av}}{S'} r^2[N_0'(r^3,t) - N_1'(r^3,t)]$$

A similar analysis for the inactive particles leads to

$$\frac{\partial N_0'(r^3,t)}{\partial t} = R\frac{4\pi N_{Av}}{S'} r^2[N_1'(r^3,t) - N_0'(r^3,t)]$$

where there is no partial derivative with respect to (r^3) because inactive particles cannot grow until they become active. Implicit in the active particle relationship is the assumption that the volume fraction of monomer θ is not a function of particle size in the range of interest.[10]

Before proceeding with the rest of the analysis, it is useful to put the population balances in dimensionless form. This is accomplished by choosing ρ as the dimensionless size parameter and dividing the expressions through by $Km_0(1-\theta)/(\theta r_m^3)$, where m_0 is the initial number of micelles, expressed as moles per liter of water. Thus

$$\rho \equiv r/r_m$$

$$\tau \equiv t(d_m/d_p)(k_p/v_m)$$

where

$$v_m \equiv (4/3)\pi r_m^3 N_{Av} \times 10^{-3} = \text{micelle volume, liters}$$

$$N_i \equiv r_m^3 N_i'(r^3,t)/m_0 = \text{(total number of particles)/(initial number of micelles)}$$

$$S \equiv S'/(4\pi r_m^2 N_{Av} m_0) = \text{(total surface area)/(initial surface area of micelles)}$$

Taking

$$R = 2fk_dI = 2fk_dI_0 \exp(-k_dt)$$

where I is the initiator concentration in the water phase, k_d is the decomposition rate constant, and f is the radical efficiency factor henceforth taken to be unity. Proceeding,

$$\alpha \equiv (k_d/k_p)(I_0/m_0)(d_p/d_m)v_m$$

$$\delta \equiv (k_d/k_p)(d_p/d_m)v_m$$

The dimensionless rate expressions now appear as

$$\frac{\partial N_1}{\partial \tau} = -[\theta/(1-\theta)]\frac{\partial N_1}{\partial(\rho^3)} + 2\alpha \exp(-\delta\tau)(\rho^2/S)(N_0 - N_1) \tag{3}$$

$$\frac{\partial N_0}{\partial \tau} = 2\alpha \exp(-\delta\tau)(\rho^2/S)(N_1 - N_0) \tag{4}$$

The average number of radicals per particle $\bar{n}$ is readily seen to be

$$\bar{n} = \int_1^\infty N_1 \, d(\rho^3) \Big/ \int_1^\infty (N_1 + N_0) \, d(\rho^3) \tag{5}$$

and average particle size (root-mean-cube radius, r_{RMC}) is

$$r_{RMC} = r_m \left\{ \int_1^\infty \rho^3 N \, d(\rho^3) \Big/ \int_1^\infty N \, d(\rho^3) \right\}^{1/3} \tag{6}$$

where

$$N = N_1 + N_0$$

Because the total surface area S is involved in the particle balances, it is necessary to express its time behavior. As noted in Eqs. (1) and (2),

$$S' = 4\pi r_m^2 N_{Av} m + 4\pi N_{Av} \int_{r_m^3}^\infty r^2 N'(r^3,t) \, d(r^3)$$

Normalizing S' with respect to the total initial micelle surface area, $4\pi r_m^2 N_{Av} m_0$, and incorporating the dimensionless parameters ρ and N, one obtains for the total dimensionless surface area,

$$S = (S'/4\pi r_m^2 N_{Av} m_0) = m/m_0 + \int_1^\infty \rho^2 N \, d(\rho^3) \tag{7}$$

The ratio of m/m_0 is described by X for convenience and is calculated based on the restriction that as long as any micelles remain in the system, the total surface area must be constant and equal to that provided by the initial micelle surface. This requires S to be constant at 1.0 throughout this period and thus

$$X = 1.0 - \int_1^\infty \rho N \, d(\rho^3) \tag{8}$$

On this basis the micelles are seen to disappear by supplying soap for the growing polymer particles as well as providing the source of new polymer particles. Thus the total dispersed phase surface area S remains constant as long as there are micelles in the system and then increases after that. When the micelles have been depleted, $X = 0$ and $S = \int_1^\infty \rho^2 N \, d(\rho^3)$.

The rate of conversion of monomer to polymer is one of the more important items to consider and can be simply expressed as

$$\frac{-dM}{dt} = k_p M_p \int_{r_m^3}^\infty N_1'(r^3,t) \, d(r^3)$$

where M is the number of moles of monomer in the latex expressed per liter of water and M_p is the monomer concentration within the polymer particles. M_p is equal to θ/v, where v is the molar volume of the monomer. The fractional conversion C may be written as $(M_0 - M)/M_0$, where M_0 is the initial value of M. Now

$$\frac{dC}{dt} = -\frac{1}{M_0}\frac{dM}{dt} = k_p \left(\frac{M_p}{M_0}\right) \int_{r_m^3}^\infty N_1'(r^3,t) \, d(r^3)$$

In dimensionless form this becomes

$$\frac{dC}{d\tau} = \beta\theta \int_1^\infty N_1 \, d(\rho^3) \tag{9}$$

where

$$\beta \equiv (v_m/v)(m_0/M_0)(d_p/d_m)$$

At this point we have all of the relations necessary to evaluate the kinetic behavior and particle-size-distribution development during the reaction. Those relationships are Eqs. (3)–(9). All that remains is to solve these differential equations.

Solution of Model Relationships

Equations (3)–(9) form a set of simultaneous, partial differential equations (actually integrodifferential equations) and require solution by numerical integration. The numerical techniques employed here utilize the method of characteristics[11] and are discussed in the Appendix.

Since the relationships of interest are partial differential equations, their solutions require both initial and boundary conditions. Most of these are obvious but those for the active particles are not and are developed in the Appendix.

Initial conditions at $\tau = 0$,

$$X = 1.0$$

$$C = 0$$

$$N_0 = 0 \text{ for all } \rho^3$$

$$N_1 = 2\alpha(1 - \theta)/\theta \text{ at } \rho^3 = 1$$

$$N_1 = 0 \text{ for all } \rho^3 > 1$$

Boundary conditions: at $\rho^3 = 1$ and at all times

$$N_0 = 0$$

$$N_1 = 2\alpha \exp(-\delta\tau)[(1 - \theta)/\theta](X/S)$$

As shown in the Appendix, the set of differential equations involved here are of the hyperbolic form and have the natural coordinate system described by $d(\rho^3)/d\tau = 0, \theta/(1 - \theta)$. This is to be interpreted as meaning that a stable numerical solution will be obtained as long as the solution follows the path of the natural coordinate system. This requires that the step sizes chosen for the numerical integration retain the relationship that $\Delta(\rho^3)/\Delta\tau = \theta/(1 - \theta)$ at all times. A much more detailed discussion of both stability and convergence of the numerical solutions is presented in Ref. 5.

The actual computations were accomplished using the method of lines,[12] which consists of discretizing one of the independent variables (ρ^3 in this case) by using a suitable finite difference approximation (a first-order backward difference was used here). This converts the partial differential equations into a system of difference—differential equations. The relationships were then solved at each characteristic grid point by the method of Runge-Kutta[13] as modified by Gill.[14]

Since Eq. (9) is actually an integrodifferential equation, care must be taken to evaluate the integral at each grid point. The simplicity of the trapezoid rule was made use of for this purpose.

An important point to emphasize is that in order to calculate the dimensionless

coefficients (e.g., α and δ) one needs to know the micellar radius. This radius is also the lower boundary of the particle size distribution. It can be easily calculated if one knows the surface area covered by one soap molecule, along with the number of soap molecules per micelle. Since the latter number may be in dispute, a series of computations were performed which used several different values of the latter quantity ranging between 50 and 100. These results are detailed in Ref. 5 and show that the choice of this parameter has *absolutely no effect* upon the predictions of the model. The dimensionless variables N, ρ, and τ are obviously dependent on the choice of this parameter, but the absolute number of particles N', particle size r, and reaction time are not. This stands to reason since the important physical parameter is the total surface area of the soap molecules available for particle formation.

RESULTS AND DISCUSSION

The solution of the model equations [(3)–(9)] subject to a choice of formulation and reactor conditions results in a prediction of the particle size distribution at any time during the process. This distribution would be expected to change substantially with increasing monomer conversion up until the time at which all of the remaining monomer is located within the existing polymer particles. Thus, during what is commonly referred to as phase III or interval III of emulsion polymerization, one should only expect to see a slight shrinkage of each particle (due to the higher density of most polymers as compared to their monomers) as long as there is no particle coalescence. Min and Ray[6] have included a coalescence mechanism in their models.

Aside from the particle size distribution itself, the detailed nature of the results allows a closer look at the radical distribution among particles of different sizes and also the reaction rate as a function of time. The following discussion will treat each of these items separately.

Particle Size Distributions

It is possible to develop distributions based on radius, area, or volume. Since the volume distribution is essentially equivalent to the weight distribution, it is one which will be discussed here. Beyond the graphical representation of the distribution, discussion will include the statistical aspects of the distributions. These parameters include the mean, the standard deviation (absolute and relative to the mean), and the skewness (nonsymmetry).

Typically one is concerned with the effect of changes in the recipe or temperature on the particle size distribution. Figure 1 shows the anticipated particle weight (volume) distributions for polystyrene latices at 50°C resulting from up to a 10-fold change in the initiator concentration, with all other variables held constant (see Appendix for the recipe, rate constants, and dimensionless parameters). These curves correspond to the time in the reaction where all of the styrene monomer is contained within the polymer particles. This corresponds to about 42% conversion for this set of conditions. Barring any particle coalescence, the curves would be the same at full conversion, except for a slight decrease in the mean size due to particle shrinkage as mentioned earlier. It is obvious from the curves alone that both the mean and the standard deviation decrease

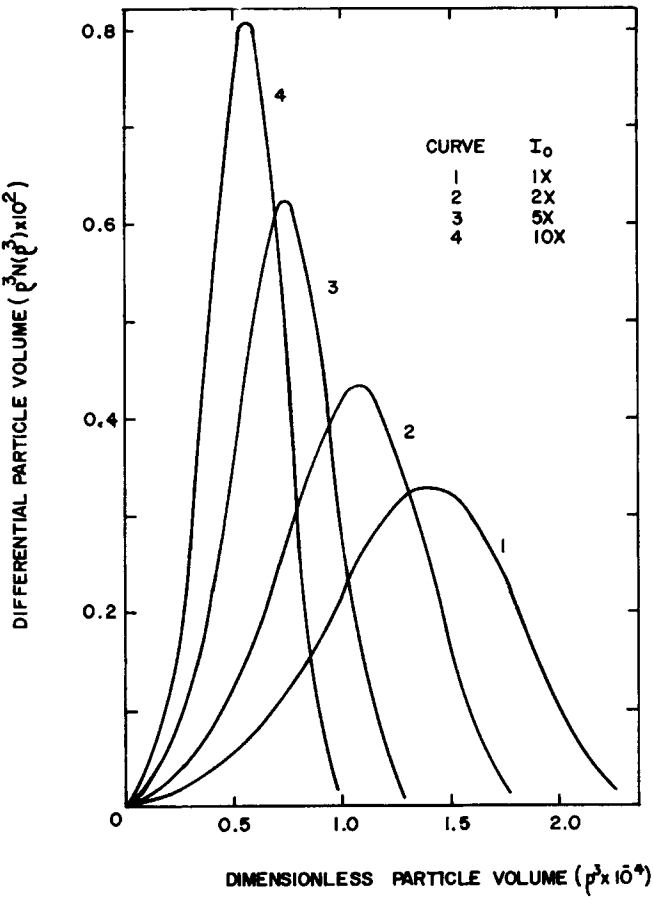

Fig. 1. Particle size distributions for various initiator levels. Recipe listed in Appendix III. Minimum value of ρ is 1.0 but it is so close to zero on this scale that the difference cannot be distinguished.

as the initiator level is increased. This behavior is as expected since the total volume of polymer particles must be the same for all the distributions (same total amount of polymer present—seen here as the same area under each curve) and at the same time there should be more particles present at the higher initiator concentrations. One additional point to note is that all of the curves are skewed toward the smallest particle size. This is seen to be the case for all conditions employing the standard batch reactor.

Figure 2 is a reproduction of experimentally measured particle size distributions obtained by Gerrens.[1] These data are for polystyrene latices polymerized at 45°C and show the results of greater than a 10-fold change in the initiator charge. Note that the results are qualitatively the same as those predicted and shown in Figure 1, including the skewness toward the small particles.

Although the predicted results are not for the same exact formulation conditions as used by Gerrens (see Appendix VI), a comparison of the statistical properties of these distributions serves to quantify these comparisons to a large extent. Table I is such a comparison for the mean particle volume (relative to

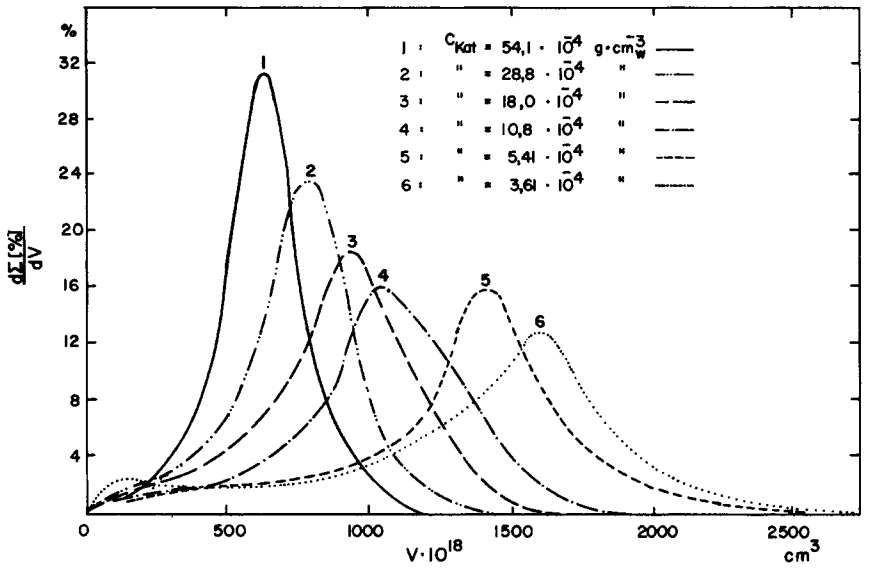

Fig. 2. Experimental particle size distributions for various initiator levels after Gerrens,[1] reproduced with permission of publisher, Springer-Verlag.

that for the base recipe), the standard deviation σ (again relative to that for the base recipe), and the coefficient of variation ν (the standard deviation expressed as a percentage of the mean). The agreement between theory and experiment is quite good and both show that the distributions become narrower on both an absolute and relative basis as the initiator level is increased.

Comparisons between theory and experiment for variations in surfactant level, temperature and monomer/water ratio are shown in Table II, with x, y, and z having the same meaning as in Table I. All of these results apply at the end of phase II when all of the monomer is contained within the polymer particles (roughly around 40% conversion for most of these cases). Attention should be paid to the direction and extent of the trends seen and not necessarily to the absolute numbers themselves, as the total recipe conditions used in the simulations did not precisely match those of Gerrens' experiments (see Appendices III and VI).

TABLE I
Effect of Initiator Level on Particle Size Distributions

A. Gerrens' data[1]				
Initiator level[a]	$1x$	$2x$	$5.3x$	$10x$
Mean volume[b]	$1.0y$	$0.790y$	$0.567y$	$0.471y$
σ[c]	$1.0z$	$0.730z$	$0.510z$	$0.369z$
ν(%)	33.8	31.3	30.4	26.5
B. Predicted results	$1x$	$2x$	$5x$	$10x$
Mean volume	$1.0y$	$0.775y$	$0.542y$	$0.412y$
σ	$1.0z$	$0.770z$	$0.532z$	$0.403z$
ν(%)	31.8	31.6	31.3	31.1

[a] x = original initiator level (slightly different for simulations and actual data).
[b] y = average particle volume for $1x$ initiator level.
[c] z = standard deviation for $1x$ initiator level.

TABLE II
Statistical Comparisons of Experimental and Predicted Distributions

A. Surfactant Level				
Gerrens' data				
Surfactant level	1x	1.87x	3.75x	7.52x
Mean volume	1.0y	0.688y	0.443y	0.241y
σ	1.0z	0.745z	0.555z	0.348z
ν(%)	37.8	40.8	47.3	54.5
Predicted results				
Surfactant level	1x	2x	4x	8x
Mean volume	1.0y	0.653y	0.398y	0.300y
σ	1.0z	0.873z	0.677z	0.545z
ν(%)	18.1	24.5	31.3	33.3
B. Temperature Level				
Gerrens' data				
Temperature (°C)	40	50	60	
Mean volume	1.0y	0.900y	0.624y	
σ	1.0z	0.676z	0.414z	
ν(%)	46.7	35.7	30.9	
Predicted results				
Temperature (°C)	40	50	60	
Mean volume	1.0y	0.565y	0.352y	
σ	1.0y	0.562z	0.346z	
ν(%)	31.4	31.3	31.0	
C. Monomer: Water Ratio				
Gerrens' data				
M:W Ratio	1:9.16	1:5.74	1:4.02	1:3.00
Mean Volume	1.0y	1.79y	2.84y	4.03y
σ	1.0z	1.69z	2.25z	2.49z
ν(%)	32.3	30.6	25.6	20.0
Predicted results				
M:W Ratio	1:2.53	1:1.85	1:1.26	1:1.01
Mean Volume	1.0y	1.41y	2.02y	2.53y
σ	1.0z	1.33z	1.83z	2.21z
ν(%)	35.0	33.3	31.9	30.7

With respect to variations in surfactant level, it can be seen from both results that while the average particle size and the standard deviation decrease with increased surfactant charge (as would naturally be expected), the distributions become significantly broader when viewed relative to the mean (i.e., ν increases). This is unlike the effect of increases in the initiator concentration and serves to underscore the independent control of each variable during the particle formation period. The reasoning behind this is that the monomer conversion at which particle formation is completed is proportional to the $^6/_5$ power of the surfactant level and to the negative $^1/_5$ power of the initiator level.[5,15] The full relation is shown as

$$C_f = K(sc)^{6/5}\left(\frac{k_p}{k_d I_0}\right)^{1/5}\left(\frac{d_p}{d_m}\right)^{4/5}\left(\frac{1}{M_0}\right) \tag{10}$$

where C_f is the fractional monomer conversion at which particle formation is complete, K is a constant, sc is the surfactant level, I_0 is the initiator level, M_0

is the overall monomer level (expressed as moles/liter of water), k_p is the propagation rate constant, k_d is the decomposition rate constant for the initiator, and d_p and d_m are the densities of the polymer and monomer, respectively. Thus while the average particle size must be smaller at higher surfactant levels (as well as the absolute standard deviation), the relative breadth of the distribution will be greater since it has been formed over a larger range of conversion. Equation (10) is the mathematical equivalent of the relation developed by Gardon[9] for P_{cr}, the volume of polymer produced up to the completion of particle nucleation.

Equation (10) is useful in interpreting the effect of temperature and monomer:water ratio as they influence the particle size distribution. It is well known that an increase in temperature decreases the average particle size and the absolute standard deviation, and Eq. (10) would indicate that when the activation energy for k_d is greater than that for k_p (as is the case for potassium persulfate and styrene) then C_f would decrease with an increase in temperature and thus produce a narrower distribution of particle sizes. This is cearly seen in both Gerrens' data and the model predictions, although the theoretical results appear to be more sensitive to temperature (for the mean and σ) than the data. This may indicate that the activation energies used in this study are somewhat incorrect.*

Increases in the latex solids content through increased monomer to water charge should produce larger particles as seen in both Gerrens' data and predictions. Because the surfactant, initiator, and temperature determine the point at which particle formation is complete, the absolute mass of polymer formed at this point should be independent of the total monomer charge.[9] Thus, when the monomer conversion is expressed as a fraction of the total monomer charge, it should decrease linearly with increasing monomer charge, as shown in Eq. (10). This suggests that the distribution should be narrower relative to the mean, but broader on an absolute basis. This behavior is clearly seen in both the experimental and theoretical results in Table II.

The significance of using σ and ν to describe the breadth of the distribution is that σ always increases with the average particle size, while ν may increase or decrease depending on which of the experimental variables are changed. The level of monomer conversion at which particle formation is complete is a useful guide to anticipating the expected change in ν.

Reaction Rates

The overall reaction rate is one of the more practical results desired from a mathematical model. Such predictions are relatively easy to check against experimental data. The analysis presented here through Eq. (9) is limited to those conditions under which every particle in the latex is allowed a maximum of a single radical. This will be the case for many small particle sized latices (and even larger ones at low initiator levels) at conversions below about 50%. For polystyrene, phase II of the reaction ends at about 40% conversion at 50°C and the following discussion will be limited to conversions below this level.

Figure 3 is a plot of calculated monomer conversion versus time (dimensionless τ) for three different surfactant levels. The recipe conditions corresponding

* k_d was taken as that value obtained in pure water while it is known, but uncharacterized, that surfactants and monomers influence the initiator dissociation reaction.[22]

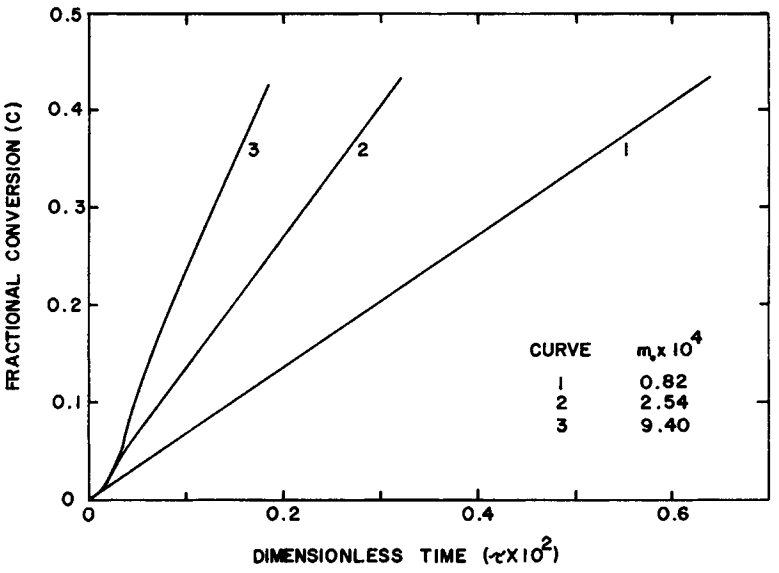

Fig. 3. Conversion profiles for various surfactant levels.

to this plot are similar to those of Figure 1 but at an initiator level of 0.27 parts and at surfactant levels of 0.90, 1.80, and 5.4 parts. The nonlinearity in these curves at low conversion has been noted by others but is somewhat difficult to show experimentally.[24] This behavior results from the fact that just after the start of the reaction there are very few particles but they all contain one radical. Much later there are many particles but on the average (see discussion of the radical distribution below) half of them contain a single radical and half contain none. Thus $\bar{n}$ starts out at 1.0 and gradually approaches 0.5. Counteracting this decrease in $\bar{n}$ is the very rapid increase in the number of particles early in the reaction and thus the reaction rate (the product of $\bar{n}$ and N') is seen to go through a maximum. This behavior is displayed in Figure 4 as a plot of the reaction rate at any time RR relative to that at the end of the phase II, RR_{II-III}. Very similar results have been shown by Gardon.[25]

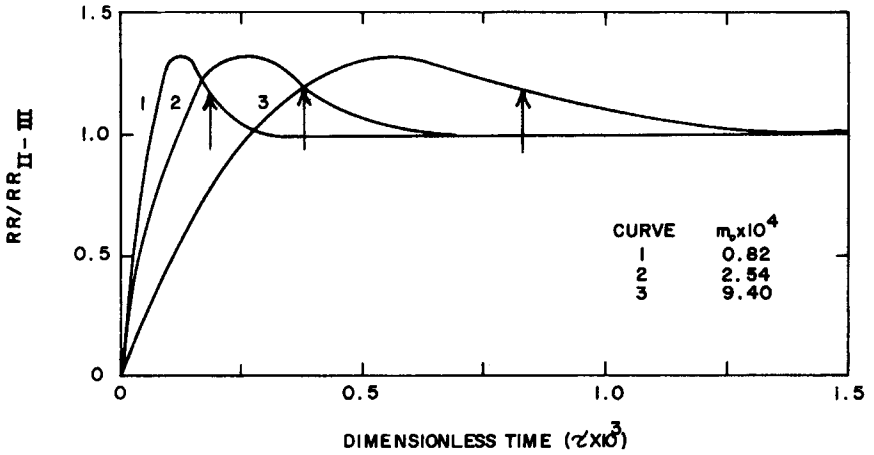

Fig. 4. Relative reaction rates for various surfactant levels. Arrows mark the end of the particle formation period.

Figure 5 shows the agreement between the model presented here and recent experimental results obtained in this laboratory by Bryers.[16] These data are for polystyrene latex produced at 50°C by the recipe noted in the figure caption. Other comparisons can be found in Ref. 5 and show good agreement between theory and experiment.

Radical Distribution Among the Particles

The type of model presented here makes it possible to obtain information regarding the number of radicals housed within particles of various sizes. These results are described as the average number of radicals per particle as a function of the particle size. Figure 6 is an example of the expected trend (at about 32%

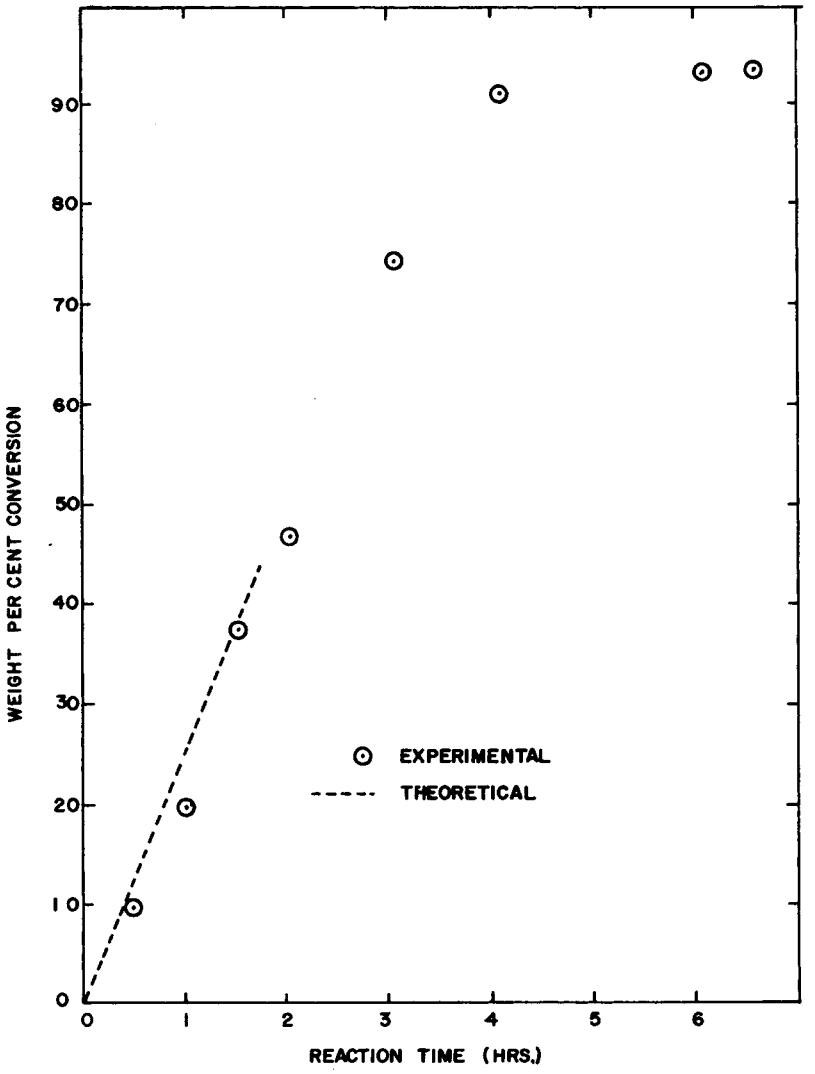

Fig. 5. Theoretical and experimental conversion profiles. Recipe—180 parts water, 100 parts styrene, 0.3 parts potassium persulfate, 1.0 parts sodium oleate.

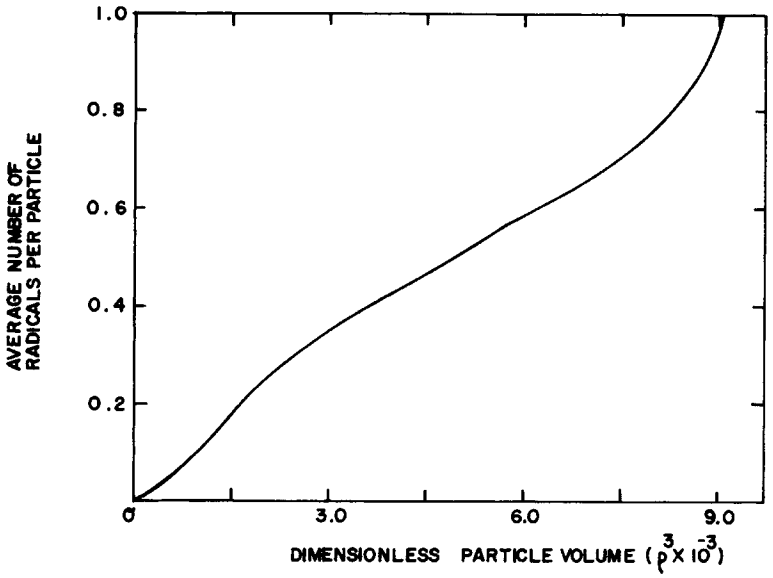

Fig. 6. Radical population versus particle size. Recipe shown in Appendix III with initiator level at 0.27 parts.

conversion, when the period of particle formation was complete at 16.5% conversion) and clearly shows that the larger particles in the system should contain a greater average number of radicals than do the smaller particles. This has an important effect on the polymer molecular weight produced in particles of different sizes, as will be discussed in a subsequent publication. The upper limit to this radical population is one per particle and is simply a result of the restriction for this model that any given particle may contain either a single radical or none at all. A similar model without this restriction is presented in Ref. 5 but its solution demands extensive computer time and memory.

The reason that the radical distribution appears as it does is because of the fact that the leading edge of the particle size distribution is controlled by the particle, which was the first to be formed and which has escaped any further entry of a free radical from the aqueous phase. Thus it has experienced a constant rate of volumetric growth throughout the polymerization reaction and only stops growing when all of the remaining monomer is contained within the polymer particles. It has therefore always had an average of one radical per particle. Following this trend backward in size, one can see that the particles at a smaller size are made up of those particles which were formed early in the reaction and did not receive a second radical (thus terminating the reaction within the particle) until late in its life, combined with those which formed later but which have sustained an uninterrupted growth. In this manner the entire radical distribution among the particles can be justified. In spite of this, it is interesting to note that when all are averaged together, the entire particle population contains on the average of one-half a radical per particle. This is subject only to the restrictions that the conversion has progressed far enough into phase II that the overall reaction rate has steadied out (refer to Fig. 4) and that any particle is limited to a maximum of one radical.

One of the results of this distribution of radicals is that the breadth of the

particle size distribution would be expected to change with increasing polymer conversion. Table III presents the statistical parameters of the expected volume distribution for a polystyrene latex at various stages of conversion. In this case, the period of particle formation was expected to be complete at about 18% conversion. The latex formulation is shown in Appendix III at 0.27 parts of initiator. As can be seen from the results, the breadth of the distribution increases significantly when viewed on an absolute basis (via σ) but actually narrows somewhat when viewed relative to the mean (ν). Also, the skewness toward the smaller sizes becomes increasingly pronounced with time. This behavior is in good agreement with the experimental results of Gardon.[23]

CONCLUDING REMARKS

It has been shown that particle size distributions calculated on the basis of Harkins' mechanism of emulsion polymerization are in reasonable agreement with experiment. Hopefully these results will strengthen the practical utilization of such mechanistic guidelines for systems similar in their behavior to polystyrene and offer a reasonable position from which to apply modifications for systems outside this range. It should not be interpreted, however, that the micellar theory of particle nucleation be accepted in its entirety, but simply that for many practical applications one can use this simple concept without deriving significant error. When working at surfactant levels close to, or below, the critical micelle concentration, these concepts will not lead to useful results. Particle nucleation in this region most likely takes place by the solution polymerization of the monomer dissolved in the water, followed by precipitation and surfactant absorption at some critical polymer length. Other contributors[9,17] have treated these areas in the past.

The author wishes to acknowledge the helpfulness and contributions of Dr. John D. Eliassen. Also, some of the reviewers' comments have been very helpful.

APPENDIX

I. Boundary and Initial Conditions for Active Particles

In order to obtain the proper boundary and initial conditions, one must consider what takes place at the lower boundary [i.e., at $(\rho^3) = 1$]. At this boundary, the particles must be of micellar size, yet in order to be polymer particles they must have or have had a radical within. However, as soon as a radical enters a micelle, the particle begins to grow away from the lower boundary. This means that there can be no inactive polymer particles at the boundary (inactive particles must have contained a radical for a finite length of time and thus have grown

TABLE III
Particle-Size-Distribution Changes with Polymer Conversion

Fraction Conversion	0.112	0.240	0.383
Mean Volume (relative)	1.0y[a]	1.98y	3.23y
σ	1.0z	1.79z	2.74z
ν(%)	37.6	33.8	31.9

[a] y and z have the same meaning as in Table I.

away from the boundary), only active polymer particles which have just that instant come from a micelle which absorbed a radical.

Performing a population balance on the active particles contained in a small size interval of width ϵ, which includes the lower boundary,

$$\frac{\partial[\epsilon N_1(1+\epsilon/2)]}{\partial\tau} = -[\theta/(1-\theta)]N_1(1+\epsilon) + 2\alpha\exp(-\delta\tau)[1+\epsilon/2]^2[N_0(1+\epsilon/2) - N_1(1+\epsilon/2)]\epsilon/S + 2\alpha\exp(-\delta\tau)X/S$$

Taking the limit of this expression as $\epsilon \to 0$, one finds that

$$N_1(1) = 2\,\alpha\exp(-\delta\tau)[(1-\theta)/\theta](X/S) \tag{A1}$$

under the conditions that $\lim_{\epsilon\to 0}[\partial N(1+\epsilon/2)/\partial\tau]$ is finite.

It is obvious from the above discussion that

$$N_0(1) = 0$$

For the initial conditions one simply sets $\tau = 0$ and $X = S = 1.0$ in Eq. (A1) and finds that

$$N(1,0) = 2\alpha(1-\theta)/\theta \tag{A2}$$

II. Coordinate System Used and Numerical Solutions

The form of the partial differential equations involved [Eqs. (3) and (4)] is determined by rewriting these equations in matrix form and following the procedure given by Ames.[11] Thus,

$$\begin{bmatrix} 1 & \theta/(1-\theta) & 0 & 0 \\ 0 & 1 & 1 & 0 \\ d\tau & d(\rho^3) & 0 & 0 \\ 0 & 0 & d\tau & d(\rho^3) \end{bmatrix} \begin{bmatrix} \partial N_1(\rho^3)/\partial\tau \\ \partial N_1(\rho^3)/\partial(\rho^3) \\ \partial N_0(\rho^3)/\partial\tau \\ \partial N_0(\rho^3)/\partial(\rho^3) \end{bmatrix} = \begin{bmatrix} 2(\alpha/S)\exp(-\delta\tau)\rho^2[N_0(\rho^3) - N_1(\rho^3)] \\ 2(\alpha/S)\exp(-\delta\tau)\rho^2[N_1(\rho^3) - N_0(\rho^3)] \\ dN_1(\rho^3) \\ dN_0(\rho^3) \end{bmatrix} \tag{A3}$$

Setting the determinant of the matrix equal to zero, one defines the "characteristic equation" as

$$\left(\frac{d(\rho^3)}{d\tau}\right)^2 - [\theta/(1-\theta)]\frac{d(\rho^3)}{d\tau} = 0$$

which is a quadratic equation in $[d(\rho^3)/d\tau]$. Solving this equation by the quadratic formula,

$$\frac{d(\rho^3)}{d\tau} = \{[\theta/(1-\theta)] \pm ([\theta/(1-\theta)]^2)^{1/2}\}/2 \tag{A4}$$

As the determinant of Eq. (A6) is positive, zero or negative, the equations are hyperbolic, parabolic or elliptic, respectively. Obviously the equations are hyperbolic in form and the "characteristic directions" are

$$\frac{d(\rho^3)}{d\tau} = [\theta/(1-\theta)], 0 \tag{A5}$$

This analysis shows that the proper coordinate system for this set of equations is ρ^3 and τ, or in dimensional form r^3 and t. It also shows that the correct step size relationship between ρ^3 and τ is to keep the ratio of step sizes equal to $\theta/(1 - \theta)$. Numerical solutions using these guidelines are seen to be stable and a discussion of convergence is given in Ref. 5.

III. Recipe Conditions for Simulations

The simulated particle size distributions shown in Figure 1 were calculated for the following conditions: water, 180 parts; styrene, 100 parts; sodium lauryl sulfate, 3.6 parts; $K_2S_2O_8$, 0.054 parts, 0.108 parts, 0.270 parts, 0.540 parts; temperature, 50°C.

IV. Rate Constants and θ

Values of the rate constants for initiator decomposition and polymer propagation were determined from published values according to Kolthoff and Miller[18] and Matheson *et al.*,[19] respectively.

At 50°C,

$$k_d = 3.64 \times 10^{-3}\ \text{hr}^{-1}\ (\text{at pH} \cong 3.5)$$

$$k_p = 4.36 \times 10^5\ \text{liter/gmol hr}$$

The appropriate activation energies were taken as 33.5 and 7.78 kcal/gmol for initiator decomposition and polymer propagation, respectively.

The volume fraction of monomer in the particles θ was taken to be 0.6.[10]

V. Micellar and Dimensionless Parameters

As noted earlier, the model utilizes a micellar radius and volume. This was done for convenience and has no effect on the computed results. For ease of computation, the number of soap molecules per micelle was chosen to be 100. The radius of the micelle was then $r_m = [100ASM/(4\pi)]^{1/2}$, where ASM is the area occupied by a single surfactant molecule when saturated on a particle surface. For sodium lauryl sulfate this value was 60 Å^2,[20,21] giving $r_m = 22$ Å. Correspondingly, $v_m = 4.4 \times 10^4$ Å^3.

The initial micellar level m_0 was calculated as $(SC\text{-}CMS)/100$. SC is the surfactant level expressed in gmoles/liter of water, CMC is the critical micelle concentration for the surfactant (9.0×10^{-3} gmol/liter of water for the sodium lauryl sulfate[20]).

Densities for the monomer and polymer were taken to be 0.88 and 1.05 g/cm^3, respectively. Using these values and the recipe conditions listed in Part III of this Appendix (for the case of 0.270 parts of initiator), the following numerical values were obtained for the various parameters of the model;

$$I_0 = 5.5 \times 10^{-3}\ \text{gmol/liter of water}$$

$$m_0 = 6.0 \times 10^{-4}\ \text{mol/liter of water}$$

$$M_0 = 5.3\ \text{gmol/liter of water}$$

$$M_p = 5.2\ \text{gmol/liter of polymer particles}$$

$$\alpha = 2.3 \times 10^{-6}$$

$$\beta = 2.9 \times 10^{-2}$$

$$\delta = 2.5 \times 10^{-7}$$

VI. Gerrens's Formulation

Gerrens's data[1] were obtained for polystyrene latices produced from recipes very similar to those used in the simulations performed here. The temperature used by Gerrens was 45°C and the type of surfactant was unspecified, except to say that it was an amphoteric soap. Potassium persulfate was used as the initiator and the basic recipe appears as water, 180 parts; styrene, 9.3 to 60 parts; soap, 0.313 to 4.2 parts; $K_2S_2O_8$ 0.065 to 0.974 parts; temperature 45°C. Gerrens' experiments were run at the following conditions (component quantities in parts and temperature in °C);

Variable	Water	Styrene	Surfactant	$K_2S_2O_8$	Temperature
Initiator	180	31.3	0.522	variable	45
Surfactant	180	31.3	variable	0.065	45
Water:monomer	180	variable	0.464	0.790	45
Temperature	180	31.3	1.05	0.065	variable

References

1. H. Gerrens, *Adv. Polymer Sci.*, **1**, 234 (1959).
2. J. L. Gardon, *J. Polym. Sci., A-1*, **6**, 665 (1968).
3. J. T. O'Toole, *J. Polym. Sci., C*, **27**, 171 (1969).
4. J. G. Watterson and A. G. Parts, *Macromol. Chem.*, **146**, 11 (1971).
5. D. C. Sundberg, Ph.D. Thesis, Univ. of Delaware (1970) and University Microfilms 71-6448.
6. K. W. Min and W. H. Ray, *J. Macromol. Sci. Rev. Macromol. Chem.*, **C11**(2), 177 (1974).
7. W. D. Harkins, *J. Chem. Phys.*, **13**, 47 (1945); **13**, 381 (1945); *J. Am. Chem. Soc.*, **69**, 1428 (1947).
8. D. W. Behnken, J. Horowitz, and S. Katz, *I&EC Fund.*, **2**, 212 (1963).
9. J. L. Gardon, *J. Polym. Sci., A-1*, **6**, 623 (1968).
10. J. L. Gardon, *J. Polym. Sci., A-1*, **6**, 643 (1968).
11. W. F. Ames, *Nonlinear Partial Differential Equations in Engineering*, Academic Press, New York, 1965, p. 416.
12. G. E. Forsythe and W. R. Wasow, *Finite Difference Method for Partial Differential Equations*, Wiley, New York, 1960, p. 178.
13. C. E. Fröberg, *Introduction to Numerical Analysis*, Addison-Wesley, Reading, MA., 1965, p. 244.
14. S. Gill, *Proc. Camb. Philos. Soc.*, **47**, 96 (1951).
15. D. C. Sundberg and J. D. Eliassen, *Polymer Colloids*, edited by R. M. Fitch, Plenum Press, New York, 1971, p. 153.
16. J. D. Bryers, M.S. Thesis, University of Idaho (1976).
17. R. M. Fitch and C. H. Tsai, *Polymer Colloids*, edited by R. M. Fitch, Plenum Press, New York, 1971, p. 73.
18. I. M. Kolthoff and I. K. Miller, *J. Am. Chem. Soc.*, **73**, 3055 (1951).
19. M. S. Matheson *et al.*, *J. Am. Chem. Soc.*, **73**, 1700 (1951).
20. H. Gerrens, *Polymer Handbook*, J. Brandrup and E. H. Immergut, Eds., Wiley, New York, 1966, p. II-399.
21. J. G. Brodnyan and G. L. Brown, *J. Colloid Sci.*, **15**, 76 (1960).
22. C. E. M. Morris and A. G. Parts, *Makromol. Chem.*, **119**, 212 (1968).
23. J. L. Gardon, *J. Polym. Sci., A-1*, **6**, 687 (1968).
24. H. M. Andersen, *J. Polym. Sci., A-1*, **7**, 2889 (1969).
25. J. L. Gardon, *J. Polym. Sci., A-1*, **9**, 2763 (1968).

Received June 30, 1977
Revised March 3, 1978